Table 2 When $\omega = 1$, the Calculation of $G(n,\omega)$ With Textual Method and Other Method

N	Re(A)	Re(B)	Im(A)	Im(B)
0	0.841470984807897	0.841470984807897	0.459697694131860	0.459697694131860
1	0.381773290676036	0.381773290676036	0.301168678939757	0.301168678939757
2	−1.44380834268741	0.239133626928383	−0.696151112779788	0.223244275483933
3	7.30097678070147	0.171738158356098	−15.8728851884444	0.177098574917010
4	170.376368986615	0.133076685139859	75.2988851973045	0.146650327556252

$$G(m+1,\omega) = \frac{e^{j\omega} - (m+1)G(m,\omega)}{j\omega} = \frac{\left[\sum_{k=0}^{m+1}(-1)^k \frac{(m+1)!}{(m+1-k)!}(j\omega)^{m+1-k}\right]e^{j\omega} + (-1)^{m+2}(m+1)!}{(j\omega)^{m+2}}$$

Finished.

It is needed to point out that when ω tends to 0 in Eq. (15), the problem of singularity still exists; therefore, the term $e^{j\omega s}$ in Eq. (14) needs to be expended in a Taylor series and then the result of integral can be gained.

With the consideration above, the final expression is given as

$$G(n,\omega) = \int_0^1 s^n e^{j\omega s} ds = \begin{cases} \dfrac{\left[\sum_{k=0}^{n}(-1)^k \dfrac{n!}{(n-k)!}(j\omega)^{n-k}\right]e^{j\omega} + (-1)^{n+1}n!}{(j\omega)^{n+1}} & |\omega| > L_t \\ \displaystyle\sum_{k=0}^{n} \frac{(j\omega)^k}{k!(k+n+1)} & |\omega| \le L_t \end{cases} \tag{16}$$

Also, L_t denotes a value close to 0. The formulas given in this paper are proved to be valid through the numerical results from the examples after.

4. NUMERICAL RESULTS

4.1. Example 1

The comparison of result from L'Hospital rule to that from textual method is given in this example.

The monostatic radar cross section (RCS) of a cone patch (Fig. 2) is computed. The cone has an upside radii of $0.5m$ and an underside radii of $1m$. The incident plane wave has a frequency of 30 MHz. Comparison of results can be seen in Figure 3.

The model used in this example is constructed by nonuniform rational B-spline and the RCS is computed by PO method. In Figure 3, the result marked A is gained from the Ludwig's algorithm that is modified by the author in this paper, namely, the result gained from formulas (9)–(11). The result marked B is gained from the Ludwig's algorithm that is modified based on the L'Hospital rule, namely, the result gained from formulas (12)–(14). The result marked C is based on triangular mesh, namely, the result gained from Eqs. (3)–(7) and (16).

From the comparison, it is shown that using the L'Hospital rule to solve the singularity problem in Ludwig's algorithm is obviously incomplete, which in reverse prove the validity of the method presented by the author in this paper.

4.2. Example 2

As the iterative formulas introduced by Fernando shows, in Eqs. (3)–(8), a value of 0.05 for L_t is enough, then the comparison of results of result from Fernando's iterative formulas to that from textual formulas is given in Table 1.

Where A represents the result form Fernando's formulas and B represents that from textual formulas. Re and Im denotes the real part and the imaginary part respectively.

It can be seen from Table 1 that when $\omega = 0.05$, instead of Fernando's description, divergence of the function appears even since $N = 2$. The function diverges seriously not only when ω is as small as 0.05 but also when ω is relatively large like $\omega = 1$, as shown in Table 2.

5. CONCLUSIONS

In PO method, Ludwig's algorithm is an important way to deal with numerical integral; however, the problem of singularity existing in the algorithm makes the application limited much, even the L'Hospital rule cannot solve the problem completely. From the numerical results presented, it is shown that the method given in this paper can solve the singularity problem in Ludwig's algorithm very well.

REFERENCES

1. A.C. Ludwig, Computation of radiation patterns involving numerical double integration, IEEE Trans Antenna Propag 11 (1968), 767–769.
2. R.J. Pogorzelski, On the Ludwig integration algorithm for triangular subregions, Proc IEEE 73 (1985), 837–838.
3. M.L.X. dos Santos and N.R Rabelo, On the Ludwig integration algorithm for triangular subregeions, Proc IEEE 74 (1986), 1455–1456.
4. F.J.S. Moreira and A. Prata, A self-checking predictor-corrector algorithm for efficient evaluation of reflector antenna radiation integrals, IEEE Trans Antenna Propag 42 (1994), 246–254.

EMC INTERNAL GSM/DCS PATCH ANTENNA FOR THIN PDA PHONE APPLICATION

Chih-Hsien Wu,[1] Kin-Lu Wong,[1] and Jeen-Sheen Row[2]

[1] Department of Electrical Engineering, National Sun Yat-Sen University, Kaohsiung 804, Taiwan

[2] Department of Electrical Engineering, National Changhua University of Education, Changhua 500, Taiwan

Received 21 June 2006

ABSTRACT: *A promising application of the electromagnetic compatible (EMC) internal patch antenna centered at the top portion of the thin smart phone or personal digital assistant (PDA) phone is presented. The EMC antenna in this study is encircled by an L-shaped shielding wall, which also serves as part of the antenna's ground plane and is centered*

above the top edge of the system ground plane. This arrangement is different from the general case of the internal patch antenna mounted on one side of the system ground plane. In this case, with the LCD monitor, battery, and associated electronic components generally mounted on both sides of the system ground plane, the required housing thickness for the PDA phone can be decreased. This makes it easy to achieve a thin PDA phone of thickness about 10 mm only. In addition, the studied antenna uses a simple radiating metal pattern of a long folded strip and a short spiral strip for generating two wide bands for GSM/DCS operation. This simple radiating metal pattern makes it easy to control the antenna's two excited resonant modes for GSM/DCS operation. Also, effects of the user's hand holding the thin PDA phone with the studied antenna are analyzed. © 2006 Wiley Periodicals, Inc. Microwave Opt Technol Lett 49: 403–408, 2007; Published online in Wiley InterScience (www.interscience.wiley.com). DOI 10.1002/mop.22167

Key words: *mobile antennas; EMC antennas; internal mobile phone antennas; thin mobile phones; user's hand*

1. INTRODUCTION

Electromagnetic compatible (EMC) internal patch antennas are mainly obtained by adding a vertical shielding metal wall, which also serves as part of the antenna's ground plane, around the side surface of the antenna [1, 2]. The shielding metal wall can effectively decrease or eliminate the possible coupling between the internal patch antenna and nearby conducting elements or electronic components in the mobile device. This property makes the impedance and radiation performances of the EMC antenna almost not affected by the nearby conducting elements [1–4]. It is thus anticipated that this kind of EMC internal patch antenna can find practical applications in mobile devices, especially when compact integration of the internal antenna and nearby electronic components inside the mobile device is desired.

In this article, we present a promising application of the EMC internal patch antenna for the thin smart phone or personal digital assistant (PDA) phone with a thickness of about 10 mm only, which is becoming very attractive for wireless users. In the proposed arrangement, the studied EMC antenna is centered above and connected to the top edge of the system ground plane of the PDA phone (see Figs. 1 and 2). This arrangement is different from the general case of the internal patch antenna mounted on one side of the system ground plane. With the proposed arrangement, the required thickness of the plastic housing for the PDA phone can be decreased, making it very promising to achieve a thin PDA phone of thickness about 10 mm only.

In the studied antenna, a simple radiating metal pattern consisting of a long folded strip and a short spiral strip is used. This simple radiating metal pattern, although in a compact configuration, can make it easy to control the antenna's two excited resonant modes at about 900 and 1800 MHz to cover the Global System for Mobile Communication (GSM, 890–960 MHz) and Digital Communication System (DCS, 1710–1880 MHz) operations. In addition, the studied EMC antenna uses a common feeding and shorting point in its radiating metal pattern, and good antenna performances over the GSM and DCS bands are obtained. This simplifies the design consideration of the antenna, since the determination of the proper distance between the feeding point and shorting point in the radiating metal pattern of conventional internal mobile phone patch antennas [5] is no longer required. Further, the case of the user's hand holding the thin PDA phone with the studied antenna is analyzed. Effects of the user's hand [6] on the antenna's impedance matching, radiation pattern, and radiation efficiency are discussed.

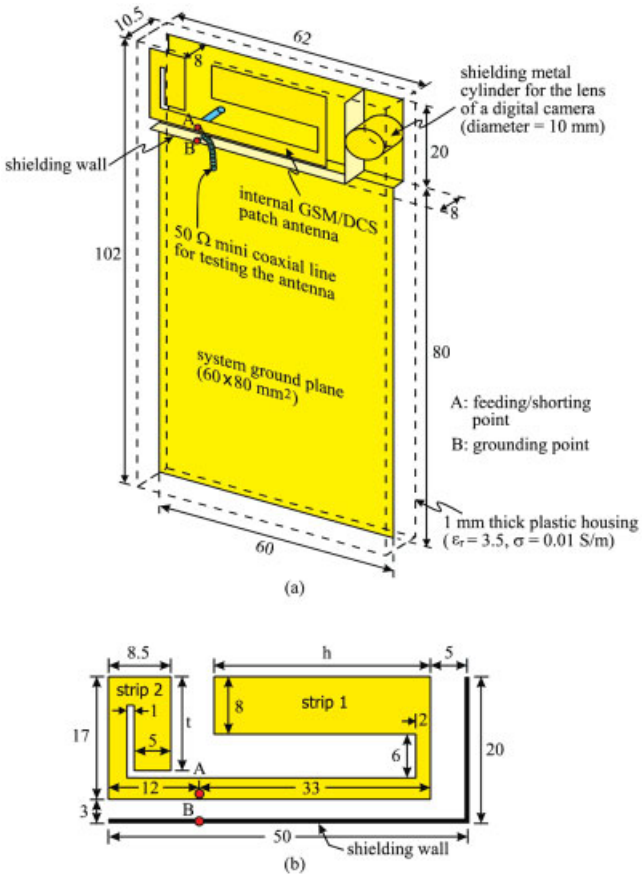

Figure 1 (a) Geometry of the studied EMC internal GSM/DCS patch antenna centered at the top portion of the thin smart phone or PDA phone. (b) Top view of the studied antenna. [Color figure can be viewed in the online issue, which is available at www.interscience.wiley.com]

2. DESIGN CONSIDERATIONS OF PROPOSED ANTENNA

Figure 1(a) shows the geometry of the studied antenna centered at the top portion of the thin PDA phone, and top view of the antenna is shown in Figure 1(b). The antenna is backed by a ground plane of 50×20 mm^2 and encircled by an L-shaped shielding metal wall of length 70 mm and height 8 mm, which also serves as part of the antenna's ground plane. The height of the shielding metal wall is the same as the thickness of the antenna or the distance between the radiating metal pattern and ground plane of the antenna. The shielding metal wall is centered above the system ground plane of dimensions 60×80 mm^2 in this study. With the proposed arrangement and the inclusion of a 1-mm thick plastic housing (relative permittivity $\varepsilon_r = 3.5$ and conductivity $\sigma = 0.01$ S/m), the thickness of the PDA phone can be about 10 mm only (see Fig. 2). As seen in the possible arrangement of the studied antenna in the thin PDA phone in Figure 2, the associated elements such as the LCD monitor, battery, keypad, and associated electronic components are mounted on both sides of the system ground plane as the general smart phones or PDA phones. Further, there is a 0.5-mm thick air gap between the antenna's radiating metal pattern and the housing's inner surface. This small air gap can effectively decrease the dielectric loading effects of the plastic housing on the radiation efficiency of the internal patch antenna, making good radiation efficiency obtained for the antenna (see the results shown in Fig. 8). The plastic housing measures 102 mm in length and 62 mm in width, which are reasonable dimensions for general PDA phones.

Also, since the studied antenna does not occupy the whole top portion of the PDA phone, an unused region of 10×20 mm^2 in

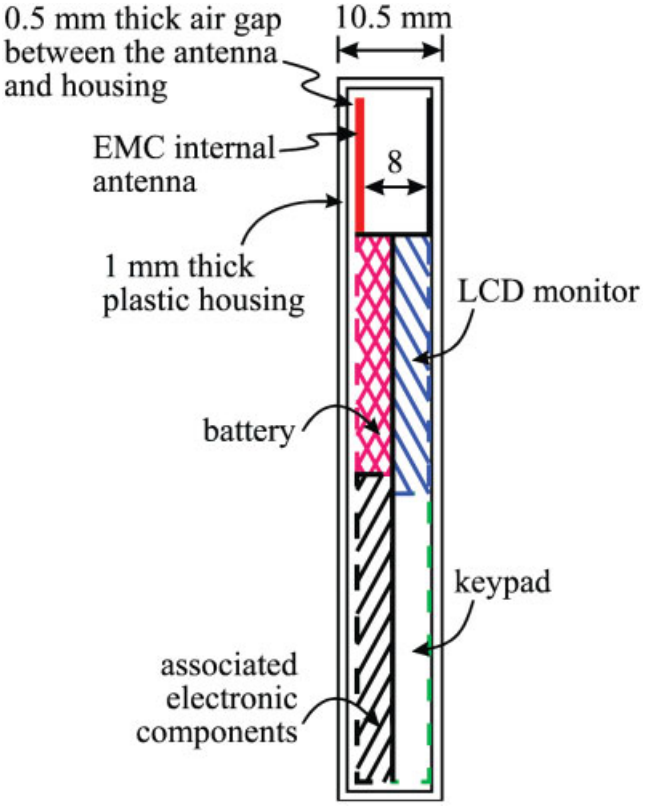

Figure 2 Possible arrangement of the studied antenna in the thin PDA phone. [Color figure can be viewed in the online issue, which is available at www.interscience.wiley.com]

the top portion [see the right top corner in the PDA phone shown in Fig. 1(a)] can be allocated for accommodating nearby electronic components. For an example, a shielding metal cylinder (diameter 10 mm here) for accommodating the lens of the digital camera [7] is installed in this unused region, which is a promising practical application.

Detailed dimensions of the antenna's radiating metal pattern are given in Figure 1(b). The metal pattern has a simple structure of comprising a long folded strip (strip 1 in the figure) and a short spiral strip (strip 2 in the figure). Both of strips 1 and 2 are short-circuited at point A (the common feeding and shorting point in the studied antenna) to the antenna's ground plane through a 8-mm long shorting post of diameter 1 mm, and are operated as quarter-wavelength structures of different lengths to control the antenna's lower and upper resonant modes, respectively. The obtained bandwidths of the two resonant modes cover the GSM and DCS operating bands. The starting portions of strips 1 and 2 are extended from point A in opposite directions, which can decrease the coupling between the two strips. In this case, the antenna's two excited resonant modes can be easily controlled separately by tuning the lengths of strips 1 and 2. However, to achieve a compact size of the radiating metal pattern, the end or open portions of strips 1 and 2 are arranged to be bent toward point A, as shown in Figure 1(b). With this compact configuration, it is still found that the antenna's two excited resonant modes can be easily controlled by first adjusting the length h (end portion of strip 1) and then the length t (end portion of strip 2). Related results will be discussed in more detail with the aid of Figures 4 and 5 in Section III. Also, in the experiment to test the antenna, a 50-Ω mini coaxial line is used across the 3-mm feed gap between point A at the radiating metal pattern and point B (the grounding point) at the shielding metal wall.

3. RESULTS OF STUDIED EMC INTERNAL ANTENNA

The EMC internal GSM/DCS patch antenna shown in Figure 1 was constructed and tested. The 1-mm thick plastic housing is included in the measurement and simulation, and the lengths h and t of the end portions of strips 1 and 2 are selected to be 30 and 13 mm, respectively. In this case, the center frequencies of the antenna's two excited resonant modes are at about 925 and 1795 MHz, center frequencies of the GSM and DCS bands. Figure 3 shows the measured and simulated return loss for the studied antenna. The simulated results are obtained using Ansoft simulation software high-frequency structure simulator (HFSS) [8]. From the results, good agreement between the measured data and simulated results is obtained. For frequencies over the GSM and DCS bands, good impedance matching (return loss better than 7.3 dB or 2.5:1 VSWR) is also achieved. This impedance matching is good for practical mobile phone applications, because the general GSM/DCS PDA phones are usually designed based on the bandwidth definition of 6 dB return loss (3:1 VSWR) only.

The antenna's two excited resonant modes can be easily adjusted by first tuning the length h (end portion of strip 1) and then the length t (end portion of strip 2). Figure 4 shows the HFSS simulated return loss as a function of h, with other parameters the same as studied in Figure 3. Results indicate that, when the length h is varied from 33 to 24 mm, the center frequency of the antenna's lower resonant mode is shifted from about 890 to 1000 MHz. Hence, one can easily tune the lower resonant mode to occur at about 925 MHz for GSM operation. Then, by tuning the length t as shown in Figure 5 with the selected length h fixed, the antenna's upper resonant mode can be varied, with the lower resonant mode almost not affected. In this case, the antenna's upper resonant mode can be tuned to occur at about 1795 MHz for DCS operation. This behavior is largely because the end portion of strip 2 is close to and faces its starting portion, and is relatively far away from all the portions of strip 1. Thus, a small variation in the length t of the end portion of strip 2 can cause only some variations in the antenna's excited upper resonant mode, with very small or almost no effects on the lower resonant mode controlled by strip 1.

Radiation characteristics of the studied antenna with $h = 30$ mm and $t = 13$ mm were also studied. Figure 6 plots the measured

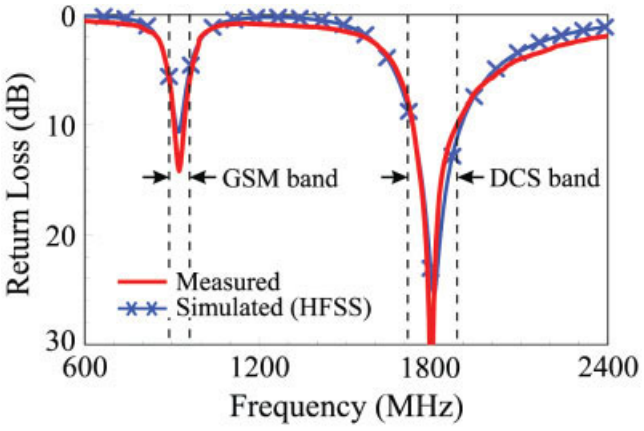

Figure 3 Measured and simulated (HFSS) return loss for the studied antenna; the 1-mm thick plastic housing ($\varepsilon_r = 3.5$, $\sigma = 0.01$ S/m) is included. [Color figure can be viewed in the online issue, which is available at www.interscience.wiley.com]

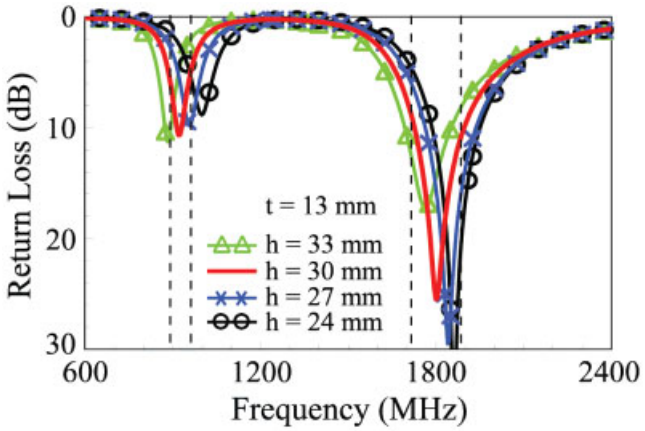

Figure 4 Simulated (HFSS) return loss as a function of h; other parameters are the same as in Figure 3. [Color figure can be viewed in the online issue, which is available at www.interscience.wiley.com]

radiation patterns at 925 MHz for the antenna with the presence of the plastic housing. The radiation patterns at 1795 MHz are shown in Figure 7. It is observed that monopole-like radiation patterns at 925 MHz are obtained, and more variations in the radiation patterns at 1795 MHz are seen. These radiation patterns show no special distinctions compared with those of the conventional internal mobile phone patch antennas [5]. The measured antenna gain and simulated radiation efficiency are shown in Figure 8. For frequencies over the GSM band shown in Figure 8(a), a stable antenna gain of about 0.5 dBi is obtained, and the radiation efficiency is close to about 60%. For frequencies over the DCS band shown in Figure 8(b), the antenna gain is also stable, about 2.5 dBi over the band, and the radiation efficiency is all larger than 85%. The obtained results indicate that good radiation characteristics are obtained for the studied antenna. When placing a conducting element or shielding metal case close to the studied antenna, very small effects on the measured return loss and radiation patterns have been observed. This behavior is the same as the EMC property reported in [1–4], and the related results are not shown here for brevity.

4. STUDY OF USER'S HAND EFFECTS

Effects of the user's hand holding the thin PDA phone with the studied EMC antenna were also analyzed. Figure 9 shows the

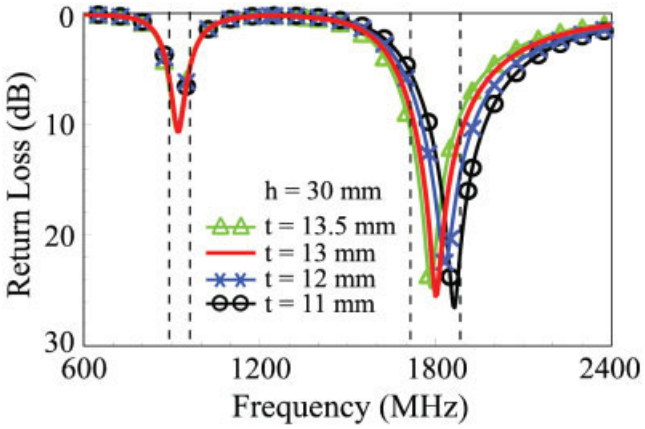

Figure 5 Simulated (HFSS) return loss as a function of t; other parameters are the same as in Figure 3. [Color figure can be viewed in the online issue, which is available at www.interscience.wiley.com]

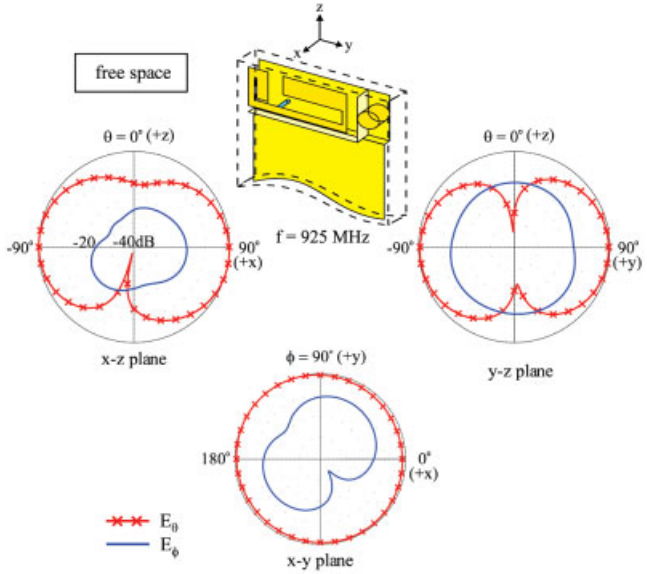

Figure 6 Measured radiation patterns at 925 MHz for the studied antenna in Figure 3. [Color figure can be viewed in the online issue, which is available at www.interscience.wiley.com]

simulation model and experimental photo of the user's hand holding the PDA phone. The simulation hand model is provided by the commercial EM simulation software SPEAG Simulation platform for EMC, Antenna design, and Dosimetry (SEMCAD) [9]. The related material parameters of skin (925 MHz: $\varepsilon_r = 41.3$, $\sigma = 0.87$ S/m; 1795 MHz: $\varepsilon_r = 38.9$, $\sigma = 1.18$ S/m), muscle (925 MHz: $\varepsilon_r = 54.9$, $\sigma = 0.95$ S/m; 1795 MHz: $\varepsilon_r = 53.6$, $\sigma = 1.34$ S/m), and bones (925 MHz: $\varepsilon_r = 20.7$, $\sigma = 0.35$ S/m; 1795 MHz: $\varepsilon_r = 19.3$, $\sigma = 0.59$ S/m) of the hand model for the study of antenna performances over the GSM and DCS bands are obtained from Ref [10]. The parameter d in the figure indicates the distance from the top edge of the thumb portion of the hand model or the real user's hand to the top edge of the plastic housing. Results of the measured

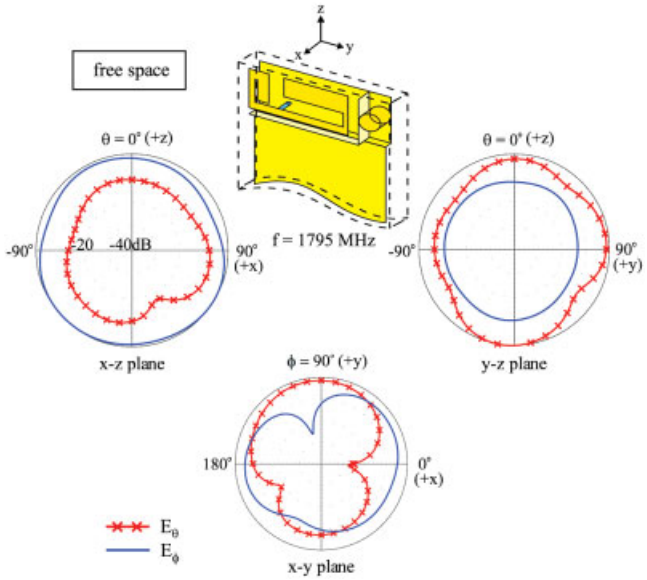

Figure 7 Measured radiation patterns at 1795 MHz for the studied antenna in Figure 3. [Color figure can be viewed in the online issue, which is available at www.interscience.wiley.com]

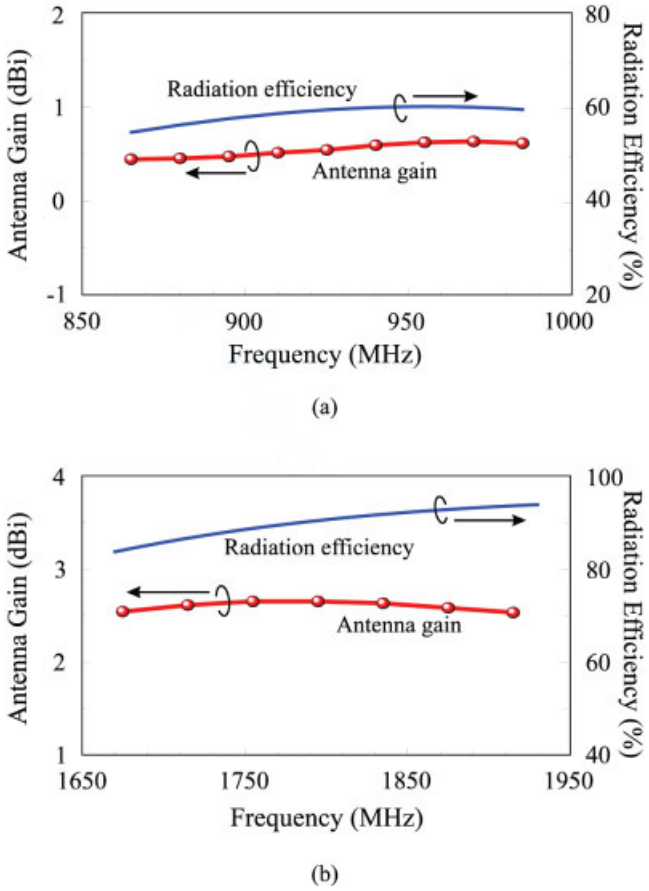

Figure 8 Measured antenna gain and simulated (HFSS) radiation efficiency for the studied antenna in Figure 3. (a) The GSM band. (b) The DCS band. [Color figure can be viewed in the online issue, which is available at www.interscience.wiley.com]

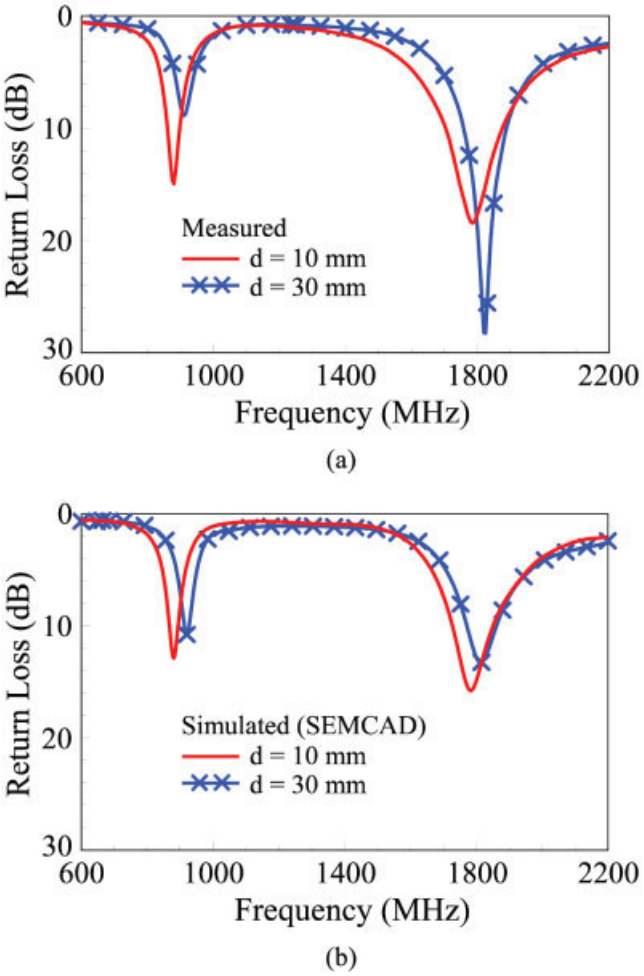

Figure 10 (a) Measured and (b) simulated (SEMCAD) return loss for $d = 10$ and 30 mm for the studied antenna with the 1-mm thick plastic housing and user's hand. [Color figure can be viewed in the online issue, which is available at www.interscience.wiley.com]

and SEMCAD simulated return loss for $d = 10$ and 30 mm for the studied antenna with the 1-mm thick plastic housing and user's hand are shown in Figure 10. From the measured data in Figure 10(a), some frequency detuning of the two excited resonant modes is seen, when the user's hand holds the PDA phone at different positions. This could cause variations in the antenna's radiation efficiency for different values of d. By comparing the simulated results in Figure 10(b) to the measured data in Figure 10(a), agreement between the measurement and simulation is also obtained.

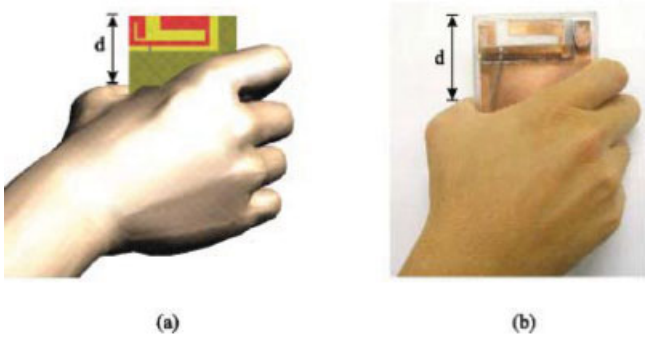

Figure 9 (a) Simulation model and (b) experimental photo of the user's hand holding the PDA phone with the studied antenna. [Color figure can be viewed in the online issue, which is available at www.interscience.wiley.com]

The SEMCAD simulated three-dimensional radiation patterns at 925 and 1795 MHz for the studied antenna with the 1-mm plastic housing and user's hand are plotted in Figure 11(a) for $d = 10$ mm and in Figure 11(b) for $d = 30$ mm. For lower frequency at 925 MHz, owing to the presence of the user's hand, the radiation patterns are no longer monopole-like or omnidirectional in the azimuthal plane (x-y plane) as shown in Figure 6. It is observed that the radiating power is greatly absorbed by the user's hand in the forearm direction, especially for the case of $d = 10$ mm. For higher frequency at 1795 MHz, similar behavior is also observed, and large distortions in the radiation patterns, especially in the user's forearm direction, are seen. The SEMCAD simulated radiation efficiency as a function of d for the studied antenna is also shown in Figure 12. Large decrease in the radiation efficiency owing to the user's hand is seen, and the efficiency is decreased with a decrease in d. That is, when the holding position of the user's hand is closer to the studied antenna in the PDA phone, the decrease in the radiation efficiency is larger. For the case of 925 MHz, the radiation efficiency is decreased from about 60% for free space (without the user's hand) to about 20% for $d = 0$. On the other hand, for the case of 1795 MHz, the radiation efficiency is decreased from about 90% for free space to about 10% only for

$d = 0$. The results indicate that the user's hand effects for the antenna operating in the DCS band are much larger. This behavior is probably because strip 2 in the radiating metal pattern for controlling the antenna's upper resonant mode for DCS operation is near the edge of the PDA phone and has a smaller size, which makes it have a more overlaid portion with the user's hand, compared with the case of strip 1. These results in the larger user's hand effect observed for the antenna operating in the DCS band.

5. CONCLUSIONS

An EMC internal GSM/DCS patch antenna for thin PDA phone application has been proposed and studied. The EMC antenna uses a simple radiating metal pattern of a long folded strip and a short spiral strip for generating two resonant modes for GSM/DCS operation, and good control of the two resonant modes has been obtained. This makes the antenna easy to design for practical applications. Good radiation characteristics for the studied EMC antenna have also been achieved. Effects of the user's hand holding the thin PDA phone with the studied EMC antenna have also been studied. Large radiation power absorption in the forearm direction of the user's hand has been observed, which results in large distortion in the antenna's radiation patterns. In addition, with the presence of the user's hand, there are large decreases in the radiation efficiency for the studied EMC antenna, especially for operating in the DCS band. This suggests that the user's hand can be treated as a very lossy medium, and it has dominant effects on the radiation efficiency of the internal antenna embedded in the mobile devices.

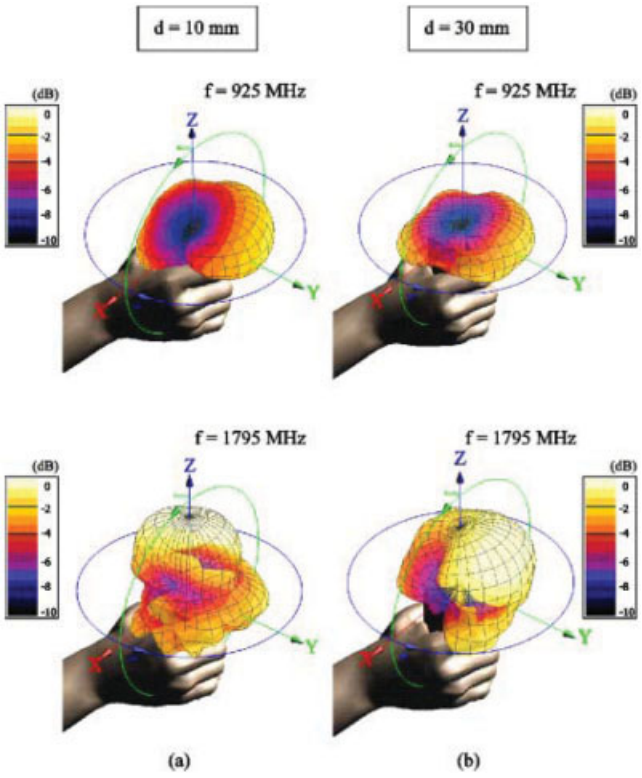

Figure 11 Simulated (SEMCAD) radiation patterns for the studied antenna with the 1-mm plastic housing and user's hand. (a) $d = 10$ mm. (b) $d = 30$ mm. [Color figure can be viewed in the online issue, which is available at www.interscience.wiley.com]

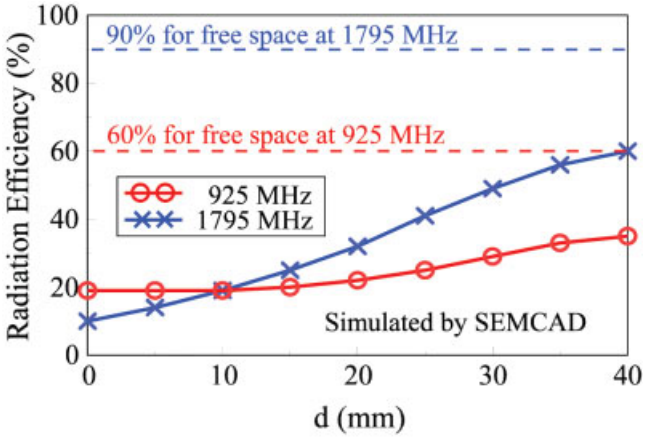

Figure 12 Simulated (SEMCAD) radiation efficiency as a function of d for the studied antenna with the 1-mm thick plastic housing and user's hand. [Color figure can be viewed in the online issue, which is available at www.interscience.wiley.com]

REFERENCES

1. C. M. Su, K. L. Wong, C. L. Tang, and S. H. Yeh, EMC internal patch antenna for UMTS operation in a mobile device, IEEE Trans Antennas Propag 53 (2005), 3836–3839.
2. K. L. Wong and C. H. Chang, Surface-mountable EMC monopole chip antenna for WLAN operation, IEEE Trans Antennas Propag 54 (2006), 1100–1104.
3. K. L. Wong, S. W. Su, C. L. Tang, and S. H. Yeh, Internal shorted patch antenna for a UMTS folder-type mobile phone, IEEE Trans Antennas Propag 53 (2005), 3391–3394.
4. K. L. Wong and C. H. Chang, WLAN chip antenna mountable above the system ground plane of a mobile device, IEEE Trans Antennas Propag 53 (2005), 3496–3499.
5. K. L. Wong, Planar antennas for wireless communications, Wiley, New York, 2003, Chap. 2.
6. C. M. Su, C. H. Wu, K. L. Wong, S. H. Yeh, and C. L. Tang, User's hand effects on EMC internal GSM/DCS dual-band mobile phone antenna, Microwave Opt Technol Lett 48 (2006), 1563–1569.
7. S. L. Chien, F. R. Hsiao, Y. C. Lin, and K. L. Wong, Planar inverted-F antenna with a hollow shorting cylinder for mobile phone with an embedded camera, Microwave Opt Technol Lett 41 (2004), 418–419.
8. Ansoft Corporation HFSS, http://www.ansoft.com/products/hf/hfss/
9. SEMCAD, Schmid & Partner Engineering AG (SPEAG), http://www.semcad.com
10. S. Gabriel, R. W. Lau, and C. Gabriel, The dielectric properties of biological tissues. III. Parametric models for the dielectric spectrum of tissues, Phys Med Biol 41 (1996), 2271–2293.